Molecular Crystals and Liquid Crystals Science and Technology. Section A. Molecular Crystals and Liquid Crystals
Publication details, including instructions for authors and subscription information:
http://www.tandfonline.com/loi/gmcl19

Surface Phenomena in Microconfined Liquid Crystals: From Cylindrical Cavities to Polymer Networks

S. Zumer [a], G. P. Crawford [b] & J. W. Doane [b]
[a] University of Ljubljana Physics Department, 61000, Ljubljana Ljubljana, Slovenia
[b] Liquid Crystal Institute Kent State University Kent, Ohio, 44242-0001, U.S.A.
Version of record first published: 23 Sep 2006.

To cite this article: S. Zumer , G. P. Crawford & J. W. Doane (1995): Surface Phenomena in Microconfined Liquid Crystals: From Cylindrical Cavities to Polymer Networks, Molecular Crystals and Liquid Crystals Science and Technology. Section A. Molecular Crystals and Liquid Crystals, 261:1, 577-592

To link to this article: http://dx.doi.org/10.1080/10587259508033499

Mol. Cryst. Liq. Cryst. 1995, Vol. 261, pp. 577–592
Reprints available directly from the publisher
Photocopying permitted by license only

SURFACE PHENOMENA IN MICROCONFINED LIQUID CRYSTALS: FROM CYLINDRICAL CAVITIES TO POLYMER NETWORKS

S. ZUMER
University of Ljubljana
Physics Department
61000 Ljubljana
Ljubljana, Slovenia

G. P. CRAWFORD AND J. W. DOANE
Liquid Crystal Institute
Kent State University
Kent, Ohio 44242-0001 U.S.A.

Abstract Confining effects of pre-filled porous matrices and anisotropic polymer networks formed during the polymerization of a small amount of prepolymer components in nematic liquid crystal matrices are studied. The pretransitional phenomena above the bulk nematic-isotropic phase transition temperature is modeled to determine the order parameter of the liquid crystal molecules at the surface of a submicrometer cylindrical cavity from magnetic resonance experiments, and to determine the order parameter of the polymer network formed in an anisotropic liquid crystal environment from birefringence measurements. From this model, we estimate the size of the internal surface of the polymer network.

INTRODUCTION

The field of liquid crystals restricted to well defined and other more complex geometries is recently attracting a lot of attention. The effect of surfaces and finite size in these systems result in a rich variety of physical phenomena: field induced structural transitions,[1] anchoring transitions,[2] deformation[3] and surface induced disordering,[4] surface induced ordering,[5] saddle-splay[6] and mixed-splay-bend[7] elasticity, defects,[8] etc. These studies are particularly stimulated by the growing number of applications involving dispersions of low molecular weight liquid crystal and polymers which belong to a broad class of composite materials. The most studied liquid crystal-polymer dispersion systems are those that consist of liquid crystal droplets embedded in a solid polymer matrix which are known as polymer dispersed liquid crystals (PDLCs).[9,10]

With small percentages of polymer, the cavities are no longer spherical in shape but become interconnected, and finally the polymer matrix is reduced to a dispersed network.[11,12] Recently, low concentration (1-5 wt. %) polymer dispersions have been exploited for many display applications; particularly those applications where bistability is a prerequisite.[13] The most impressive basic feature of low density polymer networks formed in an anisotropic liquid crystal environment is their intrinsic capability to capture and indefinitely retain the orientational order of the liquid crystal after photopolymerization.[14-16]

In contrast to the polymer dispersed liquid crystals where a structural relaxation occurs after switching the alignment with an electric field, the relaxation mechanism in polymer network systems is a volume distributed 'restoring field'. Although there are many practical uses for these dispersion materials,[11-13] the structure of dispersed polymer networks formed during polymerization in the liquid crystal phase is not completely understood despite the efforts of many researchers.[14-19] The first clues into their structures were deduced from deuterium nuclear magnetic resonance (^{2}H-NMR),[17] dielectric,[18] and diamagnetic measurements,[19] of the system before and after photopolymerization.

In this contribution we focus our attention on surface induced orientational ordering above the nematic-isotropic transition. First we briefly review results of ^{2}H-NMR studies of pretransitional nematic ordering in well defined, submicrometer cylindrical cavities[2] and then we apply a similar phenomenological description to the pretransitional ordering in polymer networks dispersed in the isotropic phase. By modeling the pretransitional behavior of the liquid crystal anchored at the polymer network, we can deduce structural features of the network in the liquid crystal.

PRETRANSITIONAL SURFACE INDUCED NEMATIC ORDERING

In the bulk isotropic phase of a liquid crystal, partial nematic order can be induced by an external magnetic or electric field. With increasing strength of the field, the first order isotropic-nematic transition can become continuous.[20] A Similar phenomenon is surface induced ordering which is localized to a thin surface layer with the thickness

comparable to the nematic correlation length.[21] Different types of ordering such as homeotropic, planar, uniaxial, biaxial, etc., exhibit different temperature and positional behaviors strongly influenced by the surface ordering field. In addition to the distinction between partial and complete wetting, prewetting transitions can also be realized.[22] This is particularly the case for degenerate planar anchoring where the ordering must undergo a symmetry breaking transition to biaxial states with the principal nematic director in the plane.[23] Here we discuss the pretransitional nematic ordering of 4'-pentyl-4-cyanobiphenyl (5CB) confined to cylindrical cavities of Anopore membranes,[2,21] and of 5CB constrained by the presence of a polymer network.

LIQUID CRYSTALS IN CYLINDRICAL CAVITIES

Anopore membranes are alumina membranes with nearly regular cylindrical cavities of radius 0.1 um which penetrate through the membrane thickness.[24] The cavities occupy approximately 30% of the volume of the membrane. The inner cavity walls have been treated with aliphatic acids of different chain lengths to promote various anchoring and ordering regimes. This is accomplished by soaking the membrane in a 4% by weight solution of an aliphatic acid (C_nH_{2n+1}-COOH) in hexane and subsequently heating the membrane for 1 hour in a vacuum oven. After the surface treatment, the membranes are filled with 5CB-αd_2 via capillary action. By varying the chain length of the aliphatic acids, the surface conditions are altered.[2] This results in an anchoring transition from planar to homeotropic anchoring at a certain length of the aliphatic chain.[2] The average ordering in the cavity is best described by the orientational wetting parameter which is defined as:[2,22]

$$\Gamma = \int_o^\infty Q(z)dz \tag{1}$$

where z measures the distance from the surface and Q is the orientational order parameter. The ^{2}H-NMR splitting originating from a given position in the cylinder is given by:[25]

$$\delta\nu = \delta\nu_o Q(\mathbf{r})(3\cos^2\theta(\mathbf{r}) - 1)/2 \quad (2)$$

where $\delta\nu_0$ is the splitting of a perfectly oriented nematic phase and $\theta(\mathbf{r})$ is the angle between the nematic director $\mathbf{n}(\mathbf{r})$ and the external magnetic field $\mathbf{B}$. Biaxial ordering has been neglcted. When the nematic correlation length, ξ, and the distance the molecules diffuse during the ^{2}H-NMR experiment, x_o, are small compared to the radius of the cavity R, the complete motional averaging limit is realized.[2,21] The average ^{2}H-NMR splitting for the magnetic field along the cylinder axis can be written as:[2,21]

$$< \delta\nu >= 2p\delta\nu_o\Gamma/R \quad (3)$$

Here p=½ for homeotropic anchoring and p =1 for parallel anchoring conditions and Q_o is the order parameter at the surface. The experimental results for two different carbon numbers n=5 and 15 indicate a strong pretansitional effect on approaching the nematic-isotropic transition temperature T_{NI} (see Fig. 1). The best description of the data is obtained if the profile of the order parameter is separated into two contributions: a surface layer of molecular thickness ξ_m where the order parameter is constant and a contribution where the order parameter is decaying according to the Landau-de Gennes theory. The thickness ξ_m for low surface order (Q_o<<1) is well approximated by $\xi_m \sim [(l^2 + 2d^2)/3]^{1/2}$ where l is the length and d the diameter of the molecule. The decay is calculated from the Landau-de Gennes free energy supplemented by the surface coupling term:[2]

$$f(Q) = a(T - T^*)Q^2/2 - bQ^3/3 + cQ^4/4 + L(dQ/dr)^2/2 + G(Q_o - Q_S)^2\delta(r - R) \quad (4)$$

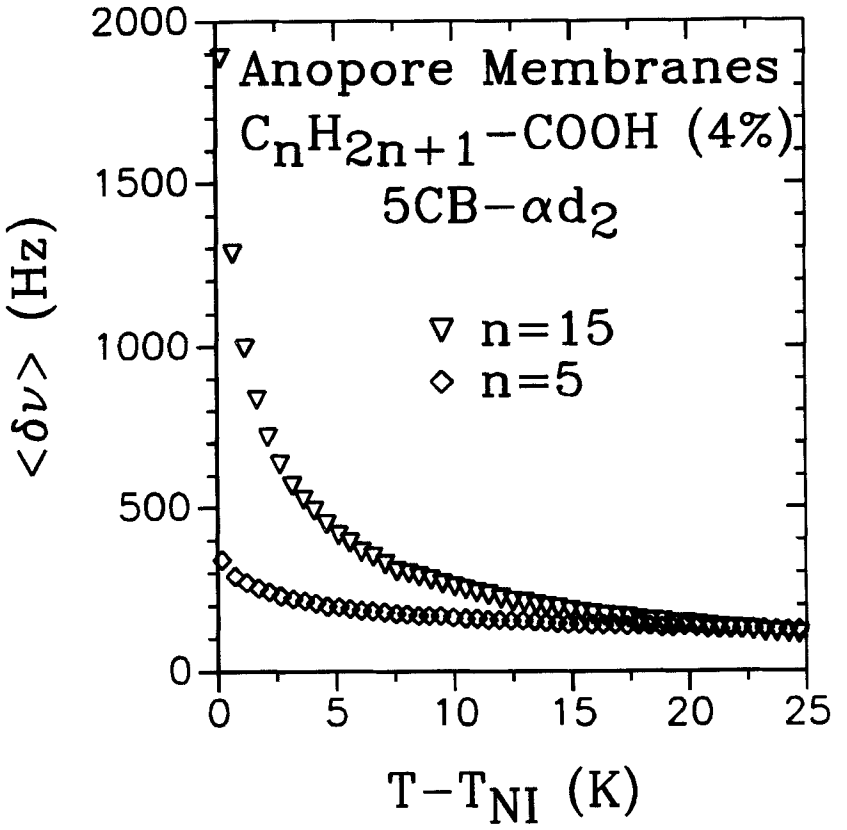

Figure 1 The averaged quadrupole splitting frequency <δν> as a function of reduced temperature T-T_{NI} for 5CB-αd_2 deuterated in the α position filled in C_nH_{2n+1}-COOH treated Anopore membranes.

where *a*, *b*, *c*, T^*, and L are conventional phenomenological coefficients, while *G* and Q_S describe the surface coupling.[2] Using 5CB values for the parameters the best fit of the data yields the parameters *G* and Q_S are summarized in the table I. The resulting values of the nematic order parameter on the surface are shown in Fig 2. Its value is smaller than the critical value 0.27 in 5CB needed for the complete wetting.[2,22] In the case n=15, it is found that Γ exhibits (or <δν>) a relatively pronounced increase as T_{NI} is approached. Therefore we use the term quasi-complete wetting[2] to distinguish the difference from the n=5 case where Q_o is practically temperature independent indicating partial wetting. Its negative value means that molecules close to the surface are

partially oriented parallel to the surface but with no preferred direction.[2] In the temperature range covered by the data there is no indication of a symmetry breaking transition.[23] It should be emphasized that weak temperature dependence of Q_0 also indicates stronger surface coupling (nearly an order of magnitude in the planar case as compared to the homeotropic case). Only a lower bound on G and Q_S are attainable for the n=5 case because of the weak temperature dependence.

Table I Estimated Interfacial parameters for the coupling between 5CB-αd_2 and C_nH_{2n+1}-COOH coated surfaces.

carbon number n	T_{NI}-T^* (K)	$G\times10^{-4}$ (J/m^2)	Q_S
5	1.5±0.2	>58.3	>-3.02
15	1.1±0.2	9.2±1.0	0.12±0.02

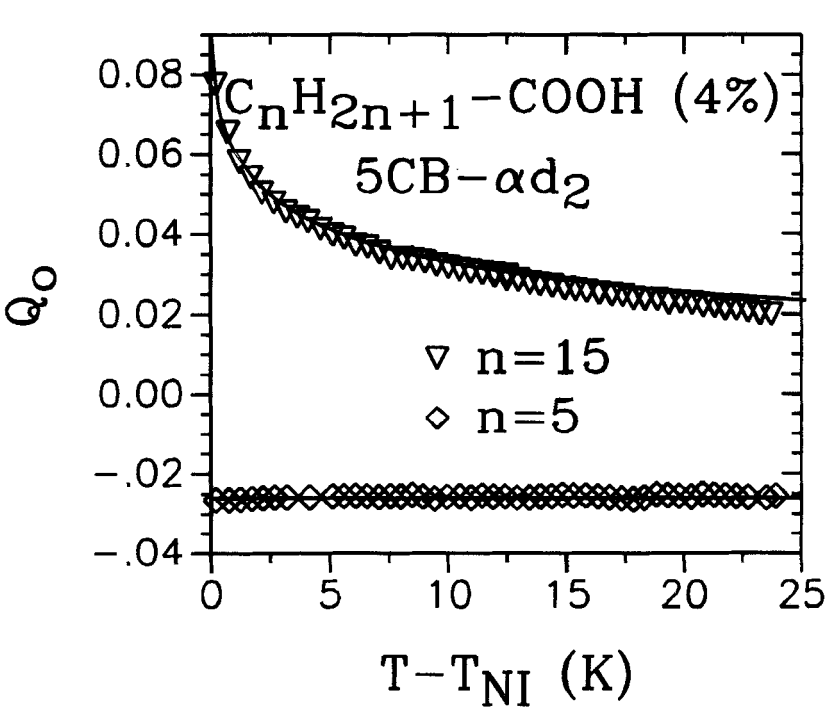

Figure 2 The surface-induced orientational order parameter Q_o as a function of reduced temperature $T-T_{NI}$ for two lengths (n) of the aliphatic acid surface aligning molecules (C_nH_{2n+1}-COOH). The solid line denotes the theoretical fit.

In all cases $Q_0 << 1$ so that the decay of Q from the surface layer of thickness ξ_m (where $\xi_m \leq z << R$) is practically exponential, $Q=Q_o \exp[(\xi_m - z)/\xi]$, yielding the expression for the averaged quadrupole splitting frequency $<\delta\nu>$:[21]

$$< \delta\nu >= 2p\delta\nu_o(\xi_m + \xi)Q_o/R \tag{5}$$

where $\xi=\xi_0[(T-T^*)/T^*]^{-1/2}$ and $\xi_0 = 0.65$ nm for 5CB.

The special behavior of the molecules in the first layer can be also deduced from the nuclear magnetic relaxation caused by the molecular exchange between the surface layer and the bulk of the liquid crystal. The relaxation causes homogeneous broadening of the ^{2}H-NMR lines in the isotropic phase. This effect is well resolved only for the case n=15 where the splitting is the largest. Using the simple line width estimate:[26]

$$\Delta = \int_0^\infty < \omega(0)\omega(t) > dt \tag{6}$$

where $\omega=\pi\delta\nu$ is the fluctuating ^{2}H-NMR quadrupolar frequency. Assuming that the molecule in the surface layer on the average stays a time τ_s, which is much longer than the time needed to cross the distance where order parameter is different from zero, we therefore can take that a molecule in time τ_s changes ω from the surface value $\pi p\delta\nu_o Q_o$ to zero (magnetic field along cylinder axis). This yields the following expression:

$$\Delta = 2(\pi p\delta\nu_o Q_o)^2 \tau_s \xi_m / R \tag{7}$$

The factor $2\xi_m/R$ results from the averaging over the cylinder. Comparing the data for the n=15 sample, one finds τ_s to be on the order of 10^{-5} s, confirming that the special state of the molecules in the surface layer is in good agreement with deuteron spin relaxation measurements on Anopore membranes. With this type of formalism we plan to estimate the network distribution in the liquid crystal environment.

POLYMER NETWORKS

Samples are prepared by dissolving 1-5 wt. % of diacrylate monomer 4,4'-bis-acryloylbiphenyl (BAB) and ~0.5 wt. % of the photoiniator benzoin methyl ether (BME) into the room temperature nematic liquid crystal 5CB. The nematic-isotropic transition temperature of bulk 5CB is 35°C. The sample is heated to 100°C and homogenized before the mixture is filled into the lecithin treated capillary tubes (diameters=100-900 mm) at ambient temperature. Cylindrical confinement was used because one can easy select a well defined nematic director-field with or without defects. We will deal with the escaped- radial director-field with and without defects, and with planar-polar director-field which are all schematically presented in Fig. 3. The capillaries are placed in a glycerin immersion to minimize refraction when optically polarizing microscopy is used. The director-field configurations in the capillary tubes prior to photopolymerization were confirmed to be the escaped-radial (splay-bend type), and in some circumstances, point defects along the cylinder axis were observed.[27] The samples were subsequently irradiated with a high pressure mercury lamp (24 mW/cm^2) at ambient temperature for ~ 40 minutes. We also stabilized the planar-polar configuration in these capillary tubes by breaking the rotational symmetry of the escaped-radial configuration with a strong electric field perpendicular to the cylinder axis. The electric field applied during photopolymerization captured the planar-polar director-field in the network.

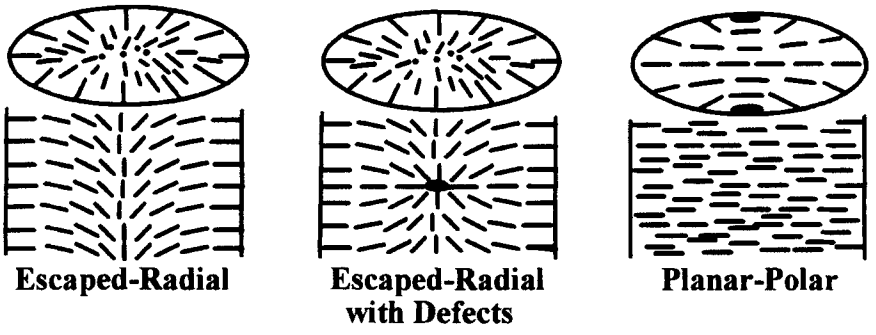

Figure 3 Three stable director-fields found in cylindrical capillaries.

A comparison of the optical birefringence texture of the escaped-radial configuration before and after photopolymerization shows a significant increase in light scattering after photo-polymerization. Therefore a disorder on the scale comparable with the wavelength of visible light is expected. This is consistent with the size of network structures observed with scanning electron microscopy when the liquid crystal was removed by evaporization. Details will be published by Fung and coworkers elsewhere.[28] At temperatures above the T_{NI} transition, a weak optical anisotropy remains and light scattering effects are minimized as presented in Fig. 4. The optical microscope textures, recorded at 25 K above the T_{NI} transition, reveal that the escaped-radial nematic director field was captured and stored by the polymer network (see Fig. 4). Also, point defects along the cylinder axis, which are otherwise metastable, have been stored as shown in Fig. 4. The observed interference colors and the lack of fringes in the cylinder with diameter 300 μm, indicate a weak optical anisotropy Δn (difference between ordinary, n_o, and extraordinary, n_e, indices of refraction) on the order of $\sim 10^{-3}$.

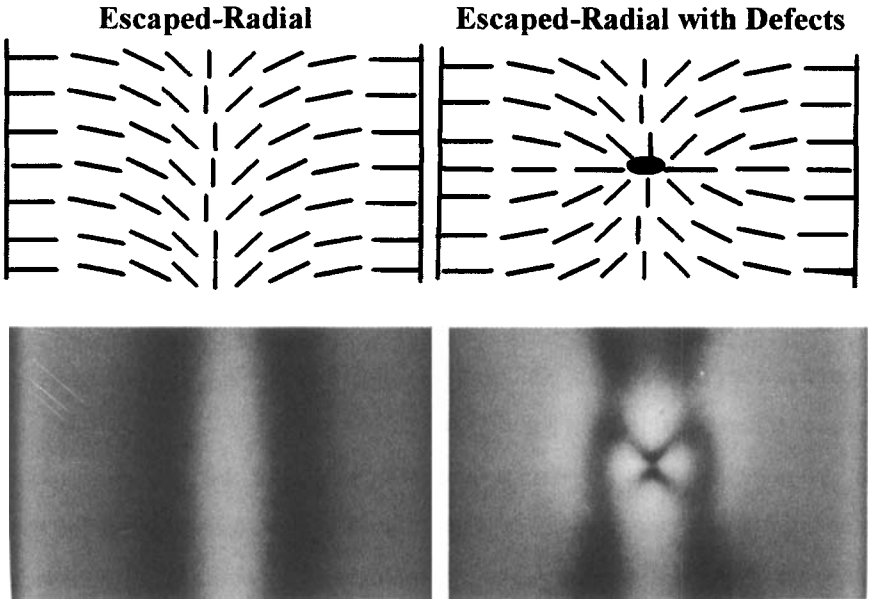

Figure 4 Optical microscope textures recorded at 25 K above the T_{NI}. The capillary axis was oriented at 45^0 between crossed polarizers. See Color Plate XIV.

To measure Δn quantitatively, we compare the data with calculated interference patterns for the homogeneously aligned planar-polar configuration. As in our previous studies we neglect diffraction and reflection effects.[30] The intensity of transmitted light, I, through the planar-polar configuration with its optical axis oriented at 45^0 with respect to the crossed polarizers is:

$$I=I_o\sin^2(\delta/2), \tag{8}$$

where $\delta=2\pi d(\mathbf{r})\Delta n(\beta)/\lambda$ is the phase shift between the ordinary and extraordinary components of light, $d(\mathbf{r})=2(R^2-r^2)^{1/2}$ is the path through the sample which depends on r, the distance from the center of the capillary, λ is the wavelength of the monochromatic light source, $\Delta n(\beta)=n_e n_o\{n_e^2\cos^2(\beta)+n_o^2\sin^2(\beta)\}^{-1/2}-n_o$ with β being the angle between the direction of observation and the orientation of the planar-polar configuration. Assuming $\Delta n=n_e-n_o<<1$, the expression for $\Delta n(\beta)$ is simplified to $\Delta n(\beta)=\Delta n\sin^2(\beta)$. Substituting the simplified expression for $\Delta n(\beta)$ into the equation for transmitted intensity I, the description of the intensity for the planar-polar configuration is given by:

$$I=I_o\sin^2[2\pi(R^2-r^2)^{1/2}\Delta n\sin^2(\beta)/\lambda], \tag{9}$$

where Δn is the only free parameter when fitting this equation to the experimental curves. The value of Δn was determined for various monomer concentrations (see Fig. 5) and temperatures (see Fig. 6). To assure reliability of the fits, the procedure was performed for different values of β between 0° and 90°.

The birefringence of the dispersions is $\sim 10^{-2}$ times that of the bulk nematic liquid crystal. There is a weak temperature dependent birefringence, more than 100 K above T_{NI}, but there is a rather strong pretransitional increase of Δn as the T_{NI} is approached from above as seen in Fig. 6. The pretransitional behavior resembles that obtained in the ^{2}H-NMR splitting in pores. This suggests that the measured Δn has two

contributions arising from the polymer network and the residual order of the liquid crystal induced by the internal surfaces of the polymer network. To separate these contributions, we extract the liquid crystal out of the network by submerging the capillary tube into a solvent (hexane). The liquid crystal is dissolved in hexane and replaced by the isotropic fluid chlorobenzene. The chlorohexane was chosen because of its relatively high boiling point and because its index of refraction is comparable to the network. No measurable swelling was detected. In addition the resubstitution of the chlorohexane with the liquid crystal yields the original texture which ensures that the network in not substantially damaged when the liquid crystal was removed and substituted by the isotropic liquid. The value of Δn for the network was estimated to be between 8×10^{-4} and 3×10^{-4} for concentrations between 4% and 1% by weight without a temperature dependence up to 130°C.

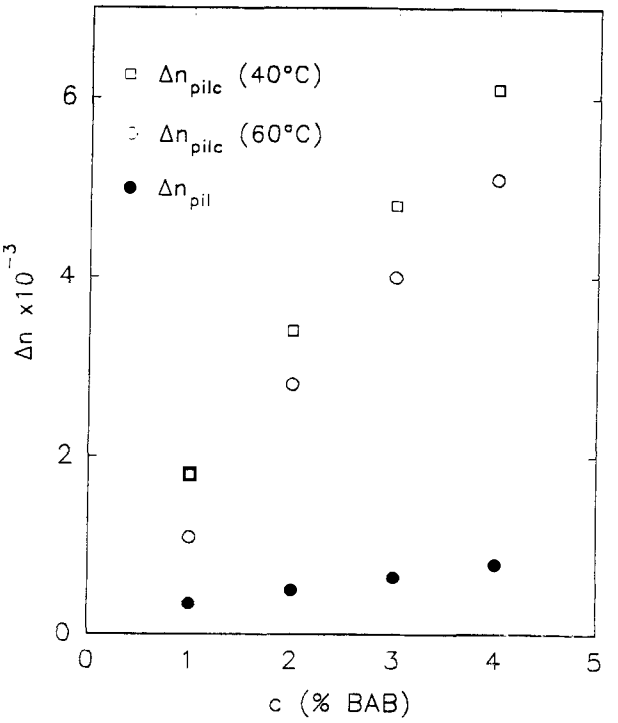

Figure 5 The optical birefringence of the polymer-liquid crystal (Δn_{pilc}) and polymer-isotropic liquid (Δn_{pil}) dispersions for a light with a wavelength of λ=589 nm as a function of concentration for two temperatures (T_{NI}=34.5°C).

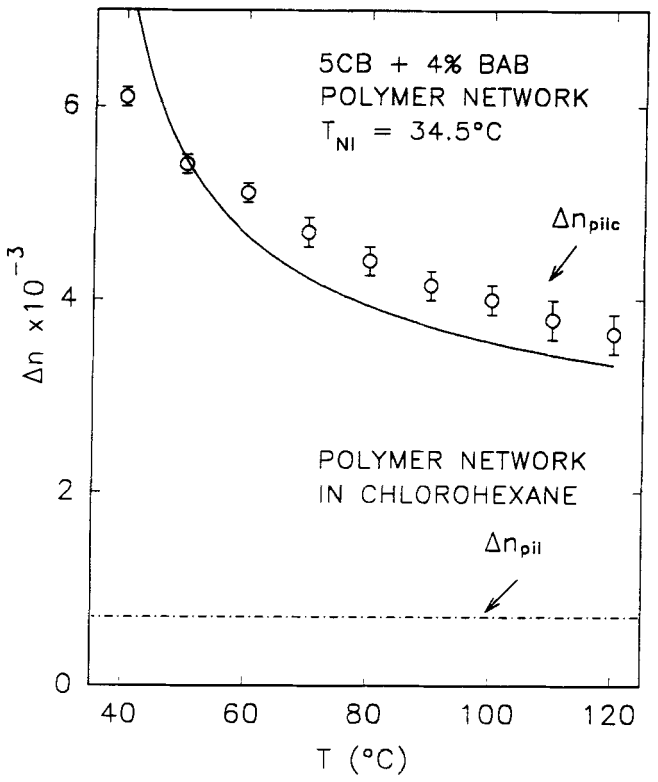

Figure 6 The optical birefringence of the polymer-liquid crystal (Δn_{pilc}) and polymer-isotropic liquid (Δn_{pil}) dispersions for a light with a wavelength of λ=589 nm as a function of temperature for the 4% concentration (T_{NI}=34.5°C).

If the differences in the index of refraction are small and of the network is well distributed in space, the refractive index of the network dispersion in the isotropic phase is $\Delta n_{pil}=cQ_p\Delta n_{op}$ where c is the percentage of polymer, and Q_p is the average order parameter of the polymer network. For our materials Δn_{op} is not known, therefore based on the chemical similarly between the polymer and liquid crystal used, we approximate Δn_{op} with the birefringence of a completely oriented liquid crystal Δn. The degree of the orientational order of the network is estimated to be between 0.08 and 0.05 depending on the concentration. The birefringence of the network dispersed

in the isotropic phase of the liquid crystal matrix, Δn_{pilc}, is a simple is a simple sum of Δn_{pil} and the contribution of the liquid crystal oriented by the network is given by:

$$\Delta n_{pilc} = \Delta n_{pil} + \Delta n_o \int_V Q(r) dV/V \tag{10}$$

where Q (r) is the local orientational order parameter of the liquid crystal and V is the volume of the system.

To simplify the calculation we use the simple exponential decay approximation for the order parameter profile that was introduced above for the porous system. The effects of the non-planar geometry are neglected in this first study which becomes less justified when the dimensions of the pockets of the network become comparable to the nematic correlation length ξ. Furthermore, the surface value of the order parameter Q_o in the surface layer of thickness ξ_m is assumed equal to Q_p; therefore the expression is given by:

$$\Delta n_{pilc} \cong \Delta n_o Q_p c[1 + (\xi_m + \xi)\alpha] \tag{11}$$

where α is the internal surface area of the network per volume of the network (A/cV). By fitting the data (see Fig. 6) by Eq. (11), we determine the only fitting parameter α to be 2 ± 1 $(nm)^{-1}$. To envision how finely the polymer network is distributed in the liquid crystal to yield such a α, we use a simple model structure (see Fig. 7) consisting of a regular square array of parallel cylindrical fibers [9]. For fibers we estimate the radius R~1 nm and their inter-fiber distance, b, is between 8 and 16 nm as c goes from 4%-to-1%. The actual structure is certainly more complex, but it should be stressed that also different model structures lead to the same conclusion: at least one dimension of the network (thickness of the fiber or layer) is comparable to typical molecular size.

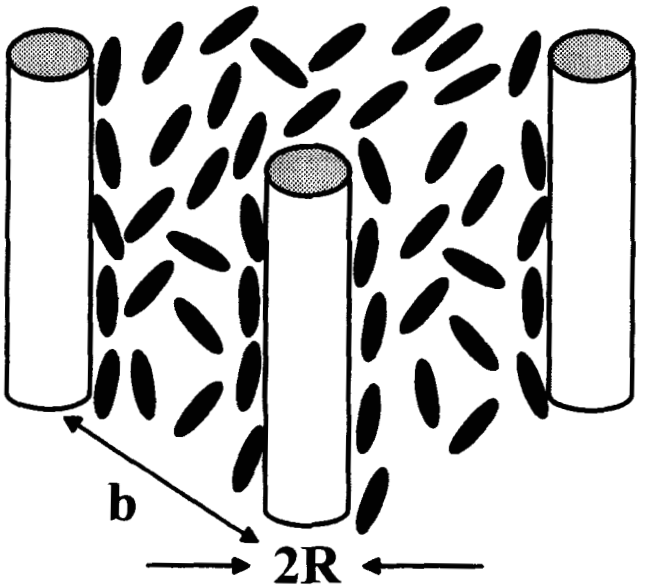

Figure 7 A model structure of the polymer network dispersed in liquid crystal.

CONCLUSIONS

We can conclude that the detailed study of the pretransitional nematic ordering in submicrometer pores with treated surfaces[2] enables us to understand the ordering effects of a polymer network dispersed in a isotropic liquid crystal. With this knowledge we have succeeded to estimate the internal surface of the low concentration network polymerized in a nematic liquid crystal matrix and to prove that the network is distributed on the molecular level. This result is in line with high percentage of bounded liquid crystal fraction found in concentrated networks. Further studies are needed to obtain more details concerning the polymer distribution to be successful in explaining the scanning electron microscope image which indicates that the network elements are inhomogeneously distributed on the micrometer scale.

ACKNOWLEDGMENTS

Research supported in part by the National Science Foundation (NSF) Science and Technology Center ALCOM DMR89-20147. The authors gratefully acknowledge discussions with Dr. Dengke Yang and Dr. L.-C. Chien.

REFERENCES

1. J. H. Erdmann, S. Zumer, and J. W. Doane, Phys Rev Lett. 64, 1907 (1990); G. P. Crawford, D. W. Allender, and J. W. Doane, Phys. Rev. A 45, 8693 (1992).
2. G. P. Crawford, R. J. Ondris-Crawford, S. Zumer and J. W. Doane, Phys. Rev. Lett. 70, 1838 (1993).
3. S. Kralj, S. Zumer, and D. W. Allender, Phys. Rev. A 43, 2943 (1991).
4. B. Barberi and G. Durand, Phys. Rev. A 41, 2207 (1990);G. S. Iannacchione and D. Finotello, Phys. Rev. Lett. 69, 2094 (1992).
5. G. P. Crawford, R. J. Ondris-Crawford, S. Zumer, and J. W. Doane, Phys. Rev. Lett. 70, 1838(1993).
6. D. W. Allender, G. P. Crawford. and J. W. Doane, Phys. Rev. Lett. 67, 1442-1445 (1991); R. D. Polak, G. P. Crawford, B. C. Kostival, J. W. Doane, and S. Zumer, Phys. Rev. E 49, R978 (1994).
7. O. D. Lavrentovich and V. M. Pergamenshchik, Phys. Rev. Lett. (to appear).
8. J. Bezic and S. Zumer, Liq. Cryst. 11, 593 (1992).
9. J. W. Doane, MRS Bulletin XVI, 22 (1991).
10. H. S. Kitzerow, Liq. Cryst. 16, 1 (1994).
11. R. A. M. Hikmet, Mol. Cryst. Liq. Cryst. 213, 117-131 (1992).
12. R. A. M. Hikmet, J. Appl. Phys. 68, 4406(1990).
13. D. K. Yang, L. C. Chien. and J. W. Doane, Proceeding of the International Display Research Conference 1, 49 (1991); D. K. Yang, L. C. Chien and J. W. Doane, Appl. Phys. Lett. 60, 3102 (1992).
14. R. A. M. Hikmet, Liq. Cryst. 9, 405-416 (1991).
15. R. A. M. Hikmet. and R. Howard, Phys. Rev. E. 48, 2752-2759 (1993).

16. G. P. Crawford, R. D. Polak, A. Scharkowski., L. C. Chien, S. Zumer and J. W. Doane , J. Appl. Phys. 75, 1968-1971 (1994).

17. R. Stannarius, G. P. Crawford, L. C. Chien, J. W. Doane, and S. Zumer, J. Appl. Phys. 75, 1968 (1994).

18. R. A. M. Hikmet and B. H. Zwerver, Liq. Cryst. 10, 835-847 (1991).

19. A. Jakli, D. Kim, L.-C. Chien and A. Saupe, J. Appl. Phys. 72, 3161-3164 (1992).

20. I. Lelidis and G. Durand, Phys. Rev. E 48, 3822 (1993).

21. G. P. Crawford, R. Stannarius, and J. W. Doane, Phys. Rev. A 44, 2558 (1991).

22. W. Chen, L. J. Martinez-Miranda, H. Hsiung, and Y. R. Shen, Phys. Rev. Lett. 62, 1860 (1989).

23. N. Kothekar, D. W. Allender, and R. M. Hornreich, Phys. Rev. E 49, 2150 (1994); Y. L'vov, R. M. Hornreich, and D. W. Allender, Phys. Rev. E 48, 1115 (1993).

24. G. P. Crawford, L. M. Stelle, R. J. Ondris-Crawford, G. S. Iannacchoine, C. J. Yeager, J. W. Doane, and D. Finotello, J. Chem. Phys. 96, 7788 (1992).

25. J. W. Doane, Magnetic Resonance of Phase Transitions, edited by F. J. Owens, C. P. Poole, Jr., and H. A. Ferach (Academic, New York, 1979) Ch. 4.

26. A. Abragam, The Princeiples of Nuclear Magnetism, (Oxford University Press, London, 1961).

27. N. Vrbancic, M. Vilfan, R. Blinc, J. Dolinsek, G. P. Crawford, and J. W. Doane, J. Chem. Phys. 98, 3540 (1993).

28. Y. Fung, S. Zumer, D. K. Yang, and J. W. Doane (to be published).

29. Y. Fung (private communication).

30. G. P. Crawford, J. A. Mitcheltree, E. P. Boyko, W. Fritz, and J. W. Doane, Appl. Phys. Lett. 60, 3226 (1992).